Impact of VCSEL Nonlinearity on Discrete MultiTone Modulation: Quasi-static Approach

F. Barrami, Yannis Le Guennec, E. Novakov, Pierre Busson

▶ **To cite this version:**

F. Barrami, Yannis Le Guennec, E. Novakov, Pierre Busson. Impact of VCSEL Nonlinearity on Discrete MultiTone Modulation: Quasi-static Approach. 21st International Conference on Telecommunications, ICT 2014, May 2014, Lisbonne, Portugal. pp.1-4. hal-01021342

HAL Id: hal-01021342
https://hal.science/hal-01021342

Submitted on 3 May 2023

HAL is a multi-disciplinary open access archive for the deposit and dissemination of scientific research documents, whether they are published or not. The documents may come from teaching and research institutions in France or abroad, or from public or private research centers.

L'archive ouverte pluridisciplinaire **HAL**, est destinée au dépôt et à la diffusion de documents scientifiques de niveau recherche, publiés ou non, émanant des établissements d'enseignement et de recherche français ou étrangers, des laboratoires publics ou privés.

Impact of VCSEL Nonlinearity on Discrete MultiTone Modulation: Quasi-static Approach

Fatima Barrami[1,2], Yannis Le Guennec[2], Emil Novakov[2] and Pierre Busson[1]
[1]STMircroelectronics Crolles, 850 rue Jean Monnet, 38920, Crolles, France
[2]IMEP-LAHC, 3 parvis Louis Neel, 38000, Grenoble, France

***Abstract*—Vertical-Cavity Surface-Emitting Lasers (VCSELs) represent many advantages for high data rate and low cost communication systems. However, they have a nonlinear transfer function, which could drastically affect the multicarrier modulations performances. The static characteristic is usually used to estimate the VCSEL nonlinearity impact on the Discrete MultiTone (DMT) modulation performances. In this paper, we demonstrate that the use of the static characteristic to model the VCSEL nonlinearity, overestimates the nonlinearity distortions when a large dynamic signal is modulating the VCSEL. In order to correctly estimate the VCSEL impact on the DMT modulation performances, we use the quasi-static characteristic to model the VCSEL nonlinearity. We show that the proposed modeling provides accurate estimations of the nonlinear distortions. The error vector magnitude (EVM) simulation results are very close to the measured EVM.**

I. Introduction

Orthogonal Frequency-Division Multiplexing (OFDM) is widely used in high data-rate radio communications because of its great immunity to inter-symbol interferences (ISI). In the last few years, there has been a great interest in OFDM for wired and wireless optical applications, due to its capacity of providing high spectral efficiency, easy implementation through digital signal processing, simple equalization, and possibility to implement bit loading algorithm for increasing capacity [1], [2].

Due to the increasing demand for end-users' bandwidth, local area networks (LANs) will have to be upgraded to support extended data rates of 40 Gbps and beyond. In existing optical wired LANs, multimode fibers (MMFs) are widely deployed as a low cost transport medium for high-speed data transmission. Optical OFDM (OOFDM) is a promising technology for short range high data communication systems such as optical wired LANs since OOFDM allows further increasing the transmission performance of legacy MMF systems, to support data rate higher than 50 Gbps over $300m$ MMF length in 99.5% of already installed MMFs [3]. For a low cost approach, Intensity Modulation Direct Detection (IM/DD) systems are preferred for both wireless and wired OFDM based optical links [4]–[6]. A real-valued baseband implementation of the OFDM modulation, called Discrete MultiTone (DMT), is commonly used in IM/DD systems. DMT is extremely sensitive to the electro-optical (E/O) converter nonlinearity and an appropriate nonlinear modeling of the (E/O) converter nonlinear behavior is required to find out the optimum operating conditions. For example, for wireless OOFDM, light emitting diodes (LEDs) are mostly used, and it has been shown that modeling LED static light-intensity (L-I) response could be a satisfying approach to simulate the LED nonlinearity and evaluate its impact on DMT waveforms [7], [8]. For wired OOFDM systems, Vertical-Cavity Surface-Emitting Lasers (VCSELs) have been recently proposed as a cost effective solution for OOFDM based IM/DD systems [6], [9]. The impact of the VCSEL nonlinearity on the DMT performances has been investigated in the literature [10]. To our knowledge, all of the presented works, have used the static light-intensity (L-I) response to evaluate the performances degradation due to the nonlinear distortions. However, in [11], we have reported that 1-dB compression point of nonlinear of VCSEL can not be correlated to the VCSEL L-I characterization, and quasi-static VCSEL characterization has been proposed to investigate the VCSEL nonlinearity.

In this paper, to the best of our knowledge, it is the first time a quasi-static model for VCSEL is used to simulate the impact of VCSEL nonlinearity on OOFDM. The simulation results obtained with the proposed model match successfully the IM/DD OOFDM experimental results. We demonstrate the relevance of the quasi-static VCSEL nonlinear model compared to the L-I response modeling.

II. VCSEL characterization and modeling

VCSELs have many advantages compared to the edge-emitting laser diodes: low threshold currents, high fiber-coupling efficiency, easy two-dimensional integration due to the surface-normal emission and the possibility of testing during the fabrication process. Due to these features, the VCSELs represent an attractive solution for high data-rate, low cost and low power communication systems. However, the VCSEL can exhibit nonlinear behavior, especially for high bias currents, due to the internal heating. The multicarrier modulations, such as OFDM and DMT have a large dynamic range making them more vulnerable to nonlinearities. In order to evaluate the impact of the VCSEL nonlinearity on the DMT performances, the VCSEL nonlinear behavior has to be characterized and modeled. The light source considered in this study is a low-cost VCSEL from Avalon photonics with an emitting wavelength of $850nm$ and a $3dB$ bandwidth from $5GHz$ to $7GHz$ for a range of DC bias currents from $3mA$ to $15mA$.

A. Static characteristic

First, the static characteristic of the light source was measured. Fig. 1 shows the measured output optical power as a function of the DC driving current. The VCSEL characteristic is measured over a range of bias currents from 0 to $15mA$, $15mA$ being the absolute maximum driving current indicated in the data sheet. As can be seen in Fig. 1, the VCSEL works with low driving currents, which could be advantageous for low-cost optical links. The threshold current of the VCSEL is $1.2mA$. For low driving currents, the L-I curve is almost linear with a slope efficiency of $0.22W/A$. For bias currents greater than $6mA$, the static characteristic exhibits a considerable nonlinearity. The nonlinear effect increases significantly with the bias current until saturation occurs at a bias current of $12mA$.

B. Quasi-static characteristic

As discussed in [11], VCSELs suffer form poor heat dissipation and consequently can exhibit strong thermally dependent behavior. In order to describe the thermal dependence of the VCSEL L-I characteristics, thermal models have been developed using modified laser rate equations [12] or multidimensional thermal heating analysis [13]. The presented models permit to accurately simulate the VCSEL's small-signal and transient behaviors, with more or less excessive levels of complexity. However, these models are valid for bias currents below the VCSEL's rollover point (I_{RO}), thereby can not be used to simulate the VCSEL's behavior when the bias current is near to the rollover point.

Motivated by the need to simulate the large-signal behavior in order to define the optimal modulation conditions, a quasi-static approach has been presented in [11]. The VCSEL quasi-static characterization consists on directly modulating the VCSEL using a sinusoidal signal at a power P_{RF}. For a given bias current and a given RF power, the minimum and maximum photodetected currents corresponding to the minimum and maximum of the modulating sinusoidal signal are measured. The corresponding optical powers are then computed using the photodiode transfer function, i.e. the photodetected current as a function of the input optical power. Thus, varying the RF power of the modulating signal, and therefore the current amplitude around the bias current, I_{DC}, a new quasi-static L-I curve permitting to describe the VCSEL large-signal behavior, can be derived. Fig. 1 compares the static and quasi-static characteristics of the Avalon Photonics VCSEL. If the VCSEL driving current is a DC current (the static curve on Fig. 1), the device temperature increases with the applied DC current causing an output optical power saturation (saturation region in Fig. 1). For DC currents higher than the rollover current ($I_{RO} \approx 15mA$), the output optical power is expected to decrease with the DC current, which corresponds to the rollover region [12], [14]. This region is not shown in Fig. 1 due to the VCSEL maximum driving current, i.e. $15mA$. On the other hand, if a dynamic signal is used to modulate the VCSEL around the DC bias current, the dynamic optical power response as function of the VCSEL driving current is almost a linear function (the quasi-static curves in Fig. 1). Indeed, when a dynamic signal is modulating the VCSEL around the DC operating current, peak amplitudes occur for a short time compared to the VCSEL semiconductor thermal time constant [15], thereby the VCSEL does not undergo any severe additional heating from the RF signal compared to the DC thermal contribution. It can be noticed as well, that the quasi-static VCSEL threshold, $I_{th,QS}$, is found to be slightly higher than the static VCSEL threshold, I_{th}. due to the fact that the VCSEL operating current induces increase of VCSEL temperature, impacting the laser threshold in dynamic regime.

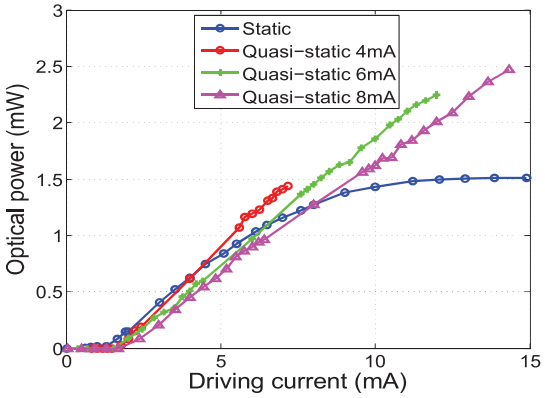

Fig. 1. The static and quasi-static characteristics of the Avalon Photonics VCSEL for different bias currents

C. VCSEL nonlinearity modeling

A simple way to model the VCSEL nonlinearity and predict its impact on a DMT system using computer simulations is the behavioral modeling approach. It consists on developing a mathematical model of the VCSEL transfer function from the measured characteristics. Therefore, contrary to the equivalent circuit modeling, the behavioral modeling approach does not require a deep knowledge of the low level circuit layout and optimizes significantly the simulation time [16]. Memory-less polynomial modeling is commonly used to represent the VCSEL nonlinear behavior [7], [8]. The accuracy of the simulation results depends on the polynomial degree. As demonstrated in [8], a second-order polynomial can provide a satisfying model for nonlinear behaviors. However, as shown in [17], the polynomial modeling with a reasonable computational complexity is not suitable for strong nonlinearities and the model represents badly the saturation region. In this paper, we use the memory-less Rapp model [18], to describe the static linear characteristic. This model is generally used in radio communications to model the power amplifier nonlinearity. The Rapp model of the VCSEL characteristic is given by

$$P_{out}(t) = G\frac{I(t) - I_{th}}{\left(1 + \left|\frac{I(t)-I_{th}}{P_{sat}/G}\right|^{2p}\right)^{1/2p}} \quad (1)$$

where P_{out} represents the output optical power, I the driving current, G the linear gain, P_{sat} the output saturation level and p is the smoothness factor. The model parameters are extracted from the input/output measurements. The parameter p permits to describe the hardness of the nonlinear characteristic. Thus, the Rapp model produces a smooth transition for the envelope characteristic as the input amplitude approaches saturation. Note that we consider that the DMT modulation signal bandwidth is smaller than the VCSEL $3dB$ bandwidth for any DC driving current in the range $3mA$ to $15mA$, so the VCSEL frequency limitation can be discarded in this model.

The N-order polynomial model of the VCSEL transfer function is given by

$$P_{out}(t) = \sum_{n=0}^{N} b_n \left[I(t)\right]^n \tag{2}$$

Fig. 2 compares the second-order polynomial and the Rapp models of the VCSEL static characteristic.

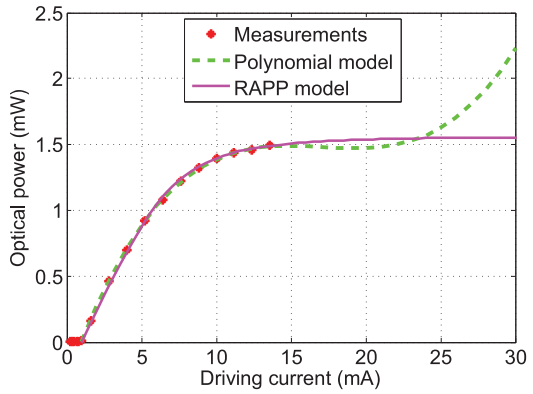

Fig. 2. Comparison of second-order polynomial and Rapp models for the VCSEL static characteristic

As can be seen in Fig. 2, both of the considered models fit correctly the measured static characteristic in the linear region. However, when the bias current exceeds the measurement range, the polynomial model increases significantly, whereas Rapp model is kept flat, simulating the saturation level. Thus, as expected, the Rapp model provides better extrapolation of the static characteristic in the saturation region than the polynomial model. As shown in Fig. 1, the VCSEL quasi-static characteristics are almost linear. Thus, a first-order polynomial can provide a satisfying model for the quasi-static transfer function.

III. Simulation Results

A. Optical link model

In this section, the impact of the VCSEL transfer function on the DMT modulation performance is investigated. The simulations are based on the simulation model shown in Fig. 3 and are carried out using Matlab software. First, in order to generate a DMT signal, the input frequency symbols to the IFFT block are constrained to have Hermitian symmetry

$$\begin{gathered} X(2N-k) = X^*(k), \quad k = 1, 2, ..., N-1 \\ X(0) = X(N) = 0 \end{gathered} \tag{3}$$

where * denotes the complex conjugation. The real time signal at the IFFT output is given by

$$x(n) = \sum_{k=0}^{2N-1} X(k) exp(j2\pi \frac{kn}{2N}) \tag{4}$$

The VCSEL is then biased at a bias I_{DC} and directly modulated using the generated DMT signal at a power P_{RF}. The resulting signal at the VCSEL output is then passed though an optical fiber and converted back to an electric signal using a PIN photodiode with a responsivity of $0.55A/W$. The DMT demodulator at the photodiode output is used to demodulate the DMT signal and recover the transmitted QAM symbols. The VCSEL is approximated by the static or quasi-static models presented in Fig. 1. The optical fiber is a standard MMF OM3 glass fiber with $50/125\mu m$ core/cladding diameters. The used fiber is quite short (i.e. $\approx 2m$), so that its impact can be neglected.

Concretely, the DMT signal has 256 subcarriers with a 16-QAM constellation. Furthermore, an oversampling with an oversampling factor of 4 is performed in order to correctly approximate the PAPR of the continuous DMT signal [19]. The error vector magnitude (EVM) metric, i.e. the difference between the received symbol and its ideal position on the constellation diagram, is used to evaluate the quality of the optical link. In this study, in order to match the measurement results, the RF power of the DMT signal is kept constant and the sweep variable is the bias current. This approach is adopted in order to overcome the limitations caused by the available equipment.

B. Optical noise components

The main noise sources in the considered optical link are the relative intensity noise (RIN) due to the spontaneous emission in the VCSEL, the shot noise due to the photodetection process and the thermal noise. The variances of the photocurrent induced by the optical noise components are given by

$$\left\langle i^2 \right\rangle_{RIN} = RIN.I_0^2.\Delta f \tag{5}$$

$$\left\langle i^2 \right\rangle_{shot} = 2qI_0.\Delta f \tag{6}$$

$$\left\langle i^2 \right\rangle_{th} = \frac{4kT\Delta f}{R_L} \tag{7}$$

where I_0 is the average photodetected current, Δf the signal bandwidth, RIN the relative intensity noise, q is the electron charge, $T(K)$ is the actual temperature, k is Boltzmann's constant and R_L is the load resistance. The total noise power at the output of the optical receiver, can be expressed as

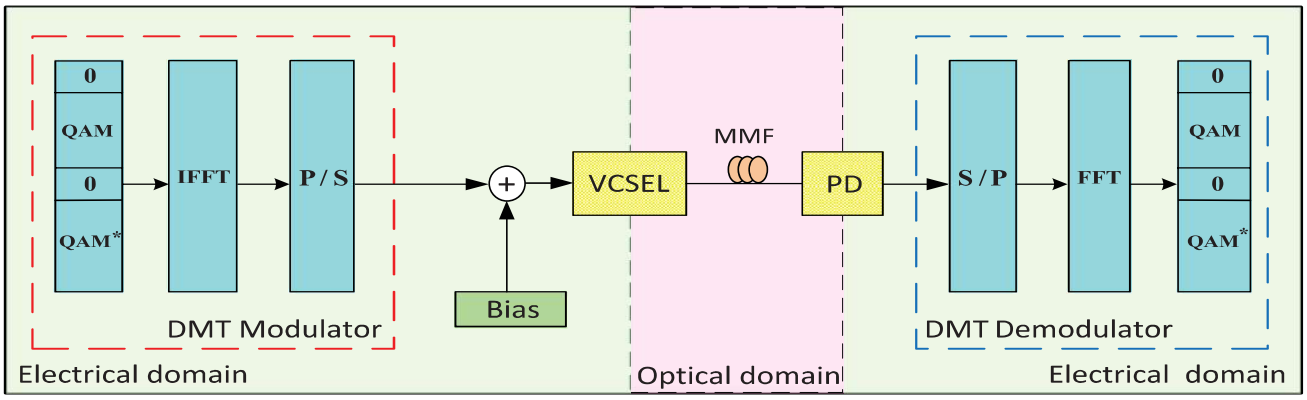

Fig. 3. Block scheme for simulations

$$P_{noise} = \left(RIN.I_0^2 + 2qI_0\right)\Delta f.R_L + 4kT\Delta f \quad (8)$$

Fig. 4 shows the contribution of each noise component to the total noise power as function of the detected photocurrent. For simplicity, the RIN noise is assumed to be a white noise with a constant value of $-125dB/Hz$, and the dark current is negligible. Thermal noise is a constant contribution versus the detected photocurrent. Shot noise has a slope of one decade/$10dB$ and RIN noise has a slope of about two decades/$10dB$. Two main regions can be defined from the results shown in Fig. 4: the first region corresponds to $I_0 < 0.01mA$, where the total noise power is dominated by the thermal noise. In the second region ($I_0 > 0.07mA$), the RIN is the dominant noise power contribution over the remaining noise components.

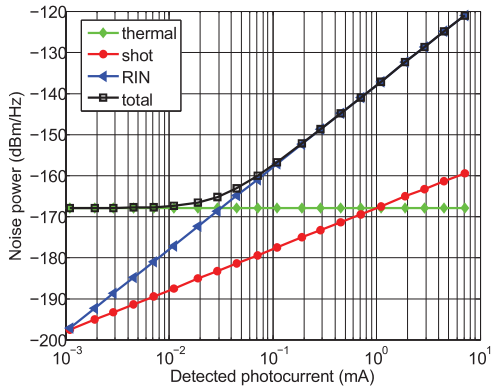

Fig. 4. Contribution of the different noise components (RIN, shot and thermal) to the total noise power as function of the detected photocurrent ($R_L = 50\Omega$)

In practice, relative intensity noise is not white noise. Furthermore, the RIN spectral density depends on the VCSEL bias current. The considered DMT signal has a bandwidth of $500MHz$. The measurements of the RIN noise in the VCSEL under test, have shown that the RIN spectral density does not exhibit important variations on the considered bandwidth. In this work, in order to take into account the dependence of the RIN noise on the frequency and the bias current, we consider the RIN mean value on the signal bandwidth for the different considered bias currents. When assuming the RIN to be the dominant noise, which is the case for the considered bias currents in this work, then the signal to noise ratio (SNR) at the receiver output can be expressed as

$$SNR_{noise} = \frac{P_{RFout}}{RIN.I_0^2.\Delta f.R_L} \quad (9)$$

where P_{RFout} is the electric power at the receiver output.

C. Nonlinearity and clipping distortions

In order to simulate the impact of the VCSEL nonlinearity on the DMT modulation, a real DMT signal is first generated using Matlab software and the bias current is added to the generated DMT signal. The nonlinearity models given in Fig. 1 are then applied to the DC biased DMT signal in order to simulate the electric optic conversion. Since the optical fiber impact and the photodiode nonlinearity are negligible, the receiver can be modeled by a linear function with a slope equal to the photodiode responsivity. The recovered QAM data at the DMT demodulator output is finally compared to the transmitted QAM data in order to compute the EVM assessing the nonlinearity and the clipping contributions to the SNR. The relationship between EVM and SNR is given by [20]

$$SNR \approx \frac{1}{EVM^2} \quad (10)$$

The SNR taking into account the VCSEL nonlinearity impact and the noise contribution, can be computed using (9) as follows

$$SNR = \frac{P_{RFout}}{P_{noise} + P_{NLD}} \quad (11)$$

$$\frac{1}{SNR} = \frac{1}{SNR_{noise}} + \frac{1}{SNR_{NLD}} \quad (12)$$

where P_{NLD} is the nonlinear distortions power and SNR_{NLD} represents the nonlinear distortion contribution to the SNR.

Let EVM_{noise} and EVM_{NLD} be respectively the EVMs due to the noise components and the nonlinear distortion. Using (10), EVM_{noise} and EVM_{NLD} can be expressed as,

$$EVM_{noise} = \sqrt{\frac{1}{SNR_{noise}}} \tag{13}$$

$$EVM_{NLD} = \sqrt{\frac{1}{SNR_{NLD}}} \tag{14}$$

Substituting (13) and (14) in (12), the total error EVM can be written as

$$EVM = \sqrt{EVM_{noise}^2 + EVM_{NLD}^2} \tag{15}$$

It has to be noted that EVM_{noise} is evaluated using the theoretical formula given by (9) and EVM_{NLD} is the simulation result of the VCSEL nonlinearity impact on the transmitted constellation using the VCSEL static and quasi-static models defined in section II. Fig. 5 shows the EVM simulation results whether the VCSEL nonlinearity is modeled by the static or the quasi-static characteristic.

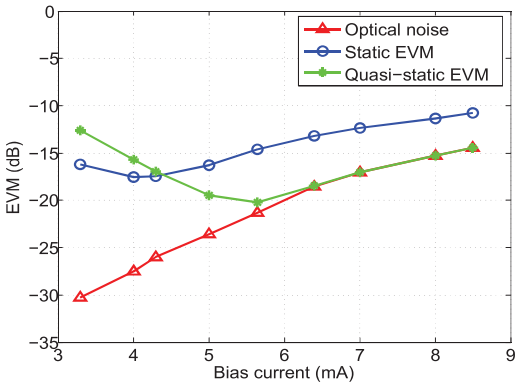

Fig. 5. Comparison of the static and quasi-static EVM simulation results as function of the VCSEL bias current

Considering the static model based on VCSEL L-I curve, for bias current $I_0 < 4.2mA$, the dominant noise is the clipping noise. For large bias currents, the optical noise and the nonlinearity distortions dominate the clipping noise. For the VCSEL quasi-static model, since the threshold ($I_{th,QS}$) is found to be lager than the static threshold (I_{th}), significant clipping noise contribution appears at larger bias current ($I_0 < 5.6mA$). For large bias currents, RIN from the laser source being the dominant noise, the signal to noise ratio, given by (12), is mainly limited by SNR_{noise}. Since, the quasi-static model is almost linear with a slope (mW/mA) larger than the static L-I response slope (Fig. 1), SNR_{noise} for the quasi-static approach is higher than for the static model. As a result, the quasi-static EVM is improved compared to the static L-I model. The optimum value for the bias current minimizing EVM is found to be significantly different considering the static model or the quasi-static model. For a given DMT signal with a given excursion, ΔI, the optimal driving current can be defined as the lowest DC bias which guarantees a minimum clipping noise. Increasing infinitely the DC bias, will increase the received photocurrent and therefore the optical noise power. The optimal driving current, $I_{DC,opt}$, that satisfies the tradeoff between the minimum clipping noise and the minimum optical noise can be expressed as

$$I_{DC,opt} - \Delta I \cong I_{th} \tag{16}$$

The considered DMT signal in both simulations and measurements has a mean power of $P_{rms} = 0.158mW$, a peak power of $P_{peak} = 1.8mW$ and a PAPR of $10.56dB$. The corresponding mean current, I_{rms}, and peak current, I_{peak}, are given by

$$I_{rms} = \sqrt{P_{rms}/R_{in}} = 1.8mA \tag{17}$$

$$I_{peak} = \sqrt{P_{peak}/R_{in}} = 6mA \tag{18}$$

where $R_{in} = 50\Omega$ is the VCSEL input resistance. The current excursion, ΔI, is then given by

$$\Delta I = I_{peak} - I_{rms} = 4.2mA \tag{19}$$

Considering the static model, the optimal current is equal to $4mA$ for a minimum EVM of $-17dB$. Substituting this current in (16) leads to

$$I_{DC,opt} - \Delta I = -0.2mA << I_{th} \tag{20}$$

The optimal driving current resulting from the use of the static model does not guarantee a minimum clipping noise, which provides an erroneous simulation of the optimal driving current. The quasi static model expects an optimal driving current of $5.65mA$ for a minimum EVM of $-20dB$. Substituting this current in (16) leads to

$$I_{DC,opt} - \Delta I = 1.45mA \cong I_{th,QS} \tag{21}$$

Equation (21) means that after adding the DC bias to the DMT signal, no peaks lower than the quasi-static threshold will remain at the VCSEL input. As a result, no clipping noise will be introduced by the VCSEL device. It has to be noted that the quasi-static approach could be used for larger bandwidths, provided that the RIN spectral density variations on the considered bandwidth are taken into account.

D. Measurements

An experimental system was built in order to experimentally validate the EVM simulation results. The experimental setup is based on the system model shown in Fig. 3. The experimental process consists on generating a real OFDM signal using Matlab software and uploading the digital signal on a Tektronix arbitrary wave generator (AWG) in order to generate a time continuous signal. The DMT frame is formed by one symbol training and four data symbols with 256 subcarriers. Furthermore, the considered oversampling reduces the noise timing jitter due to the nonideal sampling clocks [21], [22]. The guard interval is then set to zero. The sample rate of the AWG is $3GS/s$, which corresponds to

a useful bandwidth of $500MHz$, due to the oversampling and the Hermitian symmetry constraints. The time continuous signal at the AWG output is injected to the VCSEL RF input and a DC bias is added using a DC supply. At the photodiode output, an Agilent oscilloscope is used to measure the received electric OFDM signal. A channel estimation is performed offline using the training symbol. The equalization is performed in the frequency domain using a conventional zero-forcing (ZF) equalizer. Finally, the equalized OFDM data symbols are demodulated in order to recover the transmitted data and compute the EVM assessing the measured distortions.

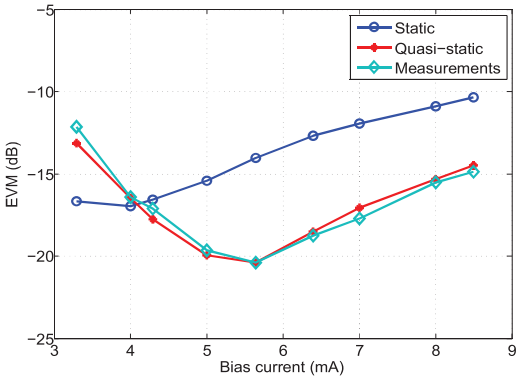

Fig. 6. Measured EVM versus the static and quasi-static EVM simulation results as function of the VCSEL bias current

Fig. 6 compares the measured EVM with the simulation results of the static and quasi-static EVMs. As expected by the theoretical analysis, modeling the VCSEL nonlinearity by the static characteristic when a large dynamic signal is used to modulate the VCSEL device, leads to inaccurate estimations of the nonlinear distortions. On the contrary, the use of the quasi-static characteristic provides a reliable estimate of the optical DMT modulation performances. The optimal driving current expected by the quasi-static model is validated by the measurements results.

IV. Conclusion

VCSELs represent a cost-effective solution for high data rate low cost optical links. The major drawback of VCSELs is their nonlinear transfer function. In order to estimate the nonlinear distortion and simulate its impact on the DMT modulation performances, the static characteristic is usually used to model the VCSEL nonlinearity. In this paper, we have demonstrated that the static characteristic is not suitable for large dynamic signals. For this reason, we have proposed to use the quasi-static characteristic to model the VCSEL nonlinearity and simulate its impact on the DMT performances in terms of EVM. The simulation results of the proposed modeling are greatly more accurate and very close to the measurement results.

References

[1] J. Armstrong, "OFDM for Optical Communications," *IEEE/OSA Journal of Lightwave Technology*, vol. 27, pp. 189-204 , 2009.

[2] E. Giacoumidis, A. Kavatzikidis, A. Tsokanos, J. M. Tang and I. Tomkos, "Adaptive Loading Algorithms for IMDD Optical OFDM PON Systems Using Directly Modulated Lasers," *IEEE Journal of Optical Communications and Networking*, Vol.4, pp. 769-778, 2012.

[3] X. Q. Jin, J. M. Tang, K. Qiu, and P. S. Spencer, "Statistical investigations of the transmission performance of adaptively modulated optical OFDM signals in multimode fibre links," *IEEE/OSA Journal of Lightwave Technology*, vol. 26, pp. 3216-3224, 2008.

[4] A. Larsson, C. Carlsson, J. Gutavsson, A. Haglund, P. Modh, A. Alping, "Broadband direct modulation of VCSELs and applications in fiberoptic links," *IEEE International Topical Meeting of Microwave Photonics*, pp. 251-254, 2004.

[5] O. Gonzalez, R. Perez-Jimenez, S. Rodriguez, J. Rabadan, and A. Ayala, "Adaptive OFDM system for communications over the indoor wireless optical channel," *IEEE Proc Optoelectronics*, vol. 153, pp. 139-144, 2006.

[6] S. C. J. Lee, F. Breyer, S. Randel, M. Schuster, J. Zeng, F. Huiskens, H. P. A. van den Boom, A. M. J. Koonen, and N. Hanik, "24-Gb/s transmission over 730 m of multimode fiber by direct modulation of 850-nm VCSEL using discrete multi-tone modulation," *IEEE/OSA Optical Fiber Communication Conference and Exposition*, paper PDP5, 2007.

[7] I. Neokosmidis, T. Kamalakis, J. W. Walewski, B. Inan, T. Sphicopoulos,"Impact of Nonlinear LED Transfer Function on Discrete Multitone Modulation: Analytical Approach," *IEEE Journat of Lightwave Technology*, vol. 27, pp. 4970-4978, 2009.

[8] B. Inan, S. C. J. Lee, S. Randel, I. Neokosmidis, A. M. J. Koonen, J.W. Walewski, " Impact of LED Nonlinearity on Discrete Multitone Modulation," *IEEE/OSA Journal Optical Communications and Networking*, vol. 1, pp. 439-451, 2009.

[9] E. Hugues-Salas, X. Q. Jin, R. P. Giddings, Y. Hong, S. Mansoor, A. Villafranca, et J. M. Tang, "Directly Modulated VCSEL-Based Real-Time 11.25-Gb/s Optical OFDM Transmission Over 2000-m Legacy MMFs," *IEEE Photonics Journal*, vol. 4, pp. 143-154, 2012.

[10] T. Cseh, T. Berceli,"Optical transmission of OFDM NQAM signals by direct laser modulation," *Microwave Radar and Wireless Communications (MIKON)*, pp. 523-526, 2012.

[11] Z. Bouhamri, Y. Le Guennec, J. Duchamp, G. Maury, B. Cabon, "Quasi-static approach to optimize RF modulation of vertical-cavity surface-emitting lasers," *Microwave Photonics (MWP)*, pp. 121-124, 2010.

[12] P. V. Mena, J. J. Morikuni, S.-M. Kang, A. V. Harton, K. W. Wyatt, "A simple rate-equation-based thermal VCSEL model," *IEEE Journat of Lightwave Technology*, Vol. 17, pp. 865-872, 1999.

[13] G. R. Hadley, K. L. Lear, M. E. Warren, K. D. Choquette, J. W. Scott, S. W. Corzine, "Comprehensive numerical modeling of vertical cavity surface-emitting lasers," *IEEE Journal of Quantum Electronics*, Vol. 32, pp. 607-616, 1996.

[14] Chen Chen, P. O. Leisher, A. A. Allerman, K. M. Geib, K. D. Choquette, "Temperature Analysis of Threshold Current in Infrared Vertical-Cavity Surface-Emitting Lasers," *IEEE Journal of Quantum Electronics*, Vol. 42, pp. 1078-1083 , 2006.

[15] A. Hangauer, J. Chen, M. C. Amann, "Square-root law thermal response in VCSELs: experiment and theoretical model," *Conference on Lasers and Electro-Optics (CLEO)*, pp. 1-2, 2008.

[16] D. Root, J. Wood, and N. Tufillaro, "New techniques for non-linear behavioral modeling of microwave/RF ICs from simulation and nonlinear microwave measurements," *Design Automation Conference*, pp. 85-90, 2003.

[17] G. Zhou, "Analysis of spectral regrowth of weakly nonlinear power amplifiers," *IEEE Communications Letters*, vol. 4, pp. 357-359, 2000.

[18] C. Rapp, "Effects of HPA-Nonlinearity on a 4-DPSK/OFDM-Signal for a Digital Sound Broadcasting System", *Second European Conference on Satellite Communications*, pp. 179-184, 1991.

[19] M. Sharif, M. Gharavi-Alkhansari, and B. H. Khalaj, "New results on the peak power of OFDM signals based on oversampling", *IEEE International Conference on Communications*, vol.2, pp. 866-871, 2002.

[20] R. A. Shafik, S. Rahman, R. Islam, "On the Extended Relationships Among EVM, BER and SNR as Performance Metrics", *International Conference on Electrical and Computer Engineering*, pp 408-411, 2006.

[21] U. Onunkwo, Y. Li, and A. Swami, "Effect of timing jitter on OFDM based UWB systems," *IEEE Journal on Selected Areas in Communications*, vol. 24, pp. 787-793, 2006.

[22] L. Yang and J. Armstrong, "Oversampling to reduce the effect of timing jitter on high speed OFDM systems", *IEEE Communications Letters*, vol. 14, pp. 196-198, 2010.